Passenger Transmitters as A Possible Cause of Aircraft Fuel Ignition

In Support of an Aircraft Accident Investigation

Truong X. Nguyen, Jay J. Ely, Kenneth L. Dudley
and Stephen A. Scearce [1]
NASA Langley Research Center, Hampton, VA
Email: truong.x.nguyen@nasa.gov

Michael O. Hatfield and Robert E. Richardson [2]
Naval Surface Warfare Center,
Dahlgren, VA

***Abstract*— An investigation was performed to study the potential for radio frequency (RF) power radiated from transmitting Portable Electronic Devices (PEDs) to create an arcing/sparking event within the fuel tank of a large transport aircraft. A survey of RF emissions from typical intentional transmitting PEDs was first performed. Aircraft measurements of RF coupling to the fuel tank and its wiring were also performed to determine the PEDs induced power on the wiring, and the re-radiated power within the fuel tank. Laboratory simulations were conducted to determine the required RF power level for an arcing/sparking event. Data analysis shows large positive safety margins, even with simulated faults on the wiring.**

Keywords- TWA-800, Aircraft Accident Investigation, Portable Electronic Devices, RF, FQIS

I. INTRODUCTION

On July 17, 1996, the Trans World Airlines Flight 800 (TWA-800) Boeing 747 Series 100 (B747-100) aircraft exploded and crashed into the Atlantic Ocean. The flight had departed 14 minutes earlier, traveling from New York's John F. Kennedy airport to Paris. To date, it is believed that a fuel vapor ignition occurred in the center-wing-tank (CWT). The cause of the ignition is still unresolved.

Approximately two years later, a special supplement was published in The New York Review of Books entitled "The Fall of TWA 800: The possibility of Electromagnetic Interference" [1]. It was a claim in this report that external RF threats, many from Department of Defense's (DoD's) high power sources on nearby ships, aircraft, and the ground contributed to the cause of the arcing event within the fuel tank. The report, along with several following papers from the same author, prefaced the desire to quantify the threat from the external high intensity radiated field (HIRF).

As a result, the DoD Joint Spectrum Center (JSC) was contracted by the National Transportation Safety Board (NTSB) to perform a detailed analysis of the TWA-800 electromagnetic environment [2]. The JSC reported that all dominant, external RF emitters were pulsed sources, with peak field intensities of up to 32.6 V/m at the time and the location of the TWA-800 event. NASA Langley Research Center (LaRC) was asked to determine if the environment could induce sufficient energy to create arcing/sparking or excessive heating on the wiring or in the fuel tank. The analysis was performed through numerical calculations analysis, and the results were reported in a different paper [3].

At the same time, NASA LaRC was also asked to determine if internal RF sources can be of concern. It can be demonstrated that a portable radio transmitting 5W may generate field levels in excess of 100 V/m close to its antenna. Inside an aircraft, these portable electronic devices (PEDs) can be placed within inches of the fuel quantity indication system (FQIS) wiring. Therefore, they can be considered a greater threat as their emissions are not subject to airframe shielding as are outside HIRF sources.

Internal PEDs sources include intentionally transmitting PEDs, such as wireless phones and two-way radios, and unintentionally transmitting devices such as laptop computers and game devices. In terms of radiated power, intentionally transmitting PEDs are much more likely to be a threat since many of them may radiate as high as 6 watts. Unintentionally transmitting devices radiate at levels below intentional radiators, even when damaged, and are not considered as a threat in this case.

This paper details the measurement, analysis and laboratory demonstration to determine the risk of transmitting PEDs to the fuel tank and its wiring, and whether there was sufficient energy in the arc/spark to be of concerns. Fig. 1 illustrates the external and internal potential RF threats. Only internal threats are considered in this paper.

II. APPROACH

PED and their RF emission envelopes were first identified. RF coupling measurements between the passenger cabin and the fuel tank and its CWT wiring were then performed on a retired Boeing 747 aircraft of the same production series. Together, these data provide an upper bound on the maximum RF threats to the fuel tank. Laboratory testing was also conducted to determine the power requirement for an arc/spark on the FQIS wiring. The safety margin was determined from the measured data.

In the laboratory testing, a fault was simulated on a set of FQIS wiring at the location determined to have the highest

[1] Stephen A. Scearce is currently with Cisco Systems Inc.
[2] Dr. Robert E. Richardson is now retired

voltage/current gain. This simulation emulated the severe conditions that include damaged wiring, or floating conducting debris in the tank that may short circuit the terminals.

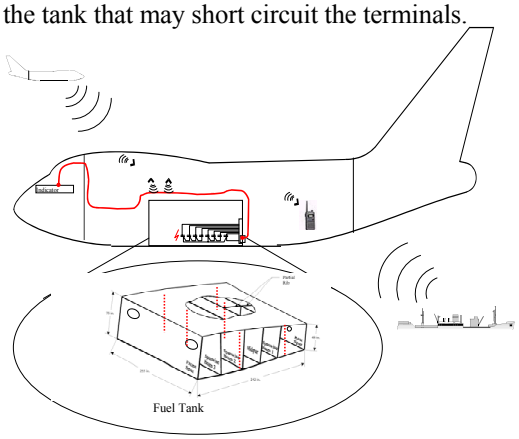

Figure 1. External and internal RF threats to a B747 fuel tank and its wiring.

III. Estimating Typical PED Threats

PED threats considered were limited to intentionally transmitting and commercially available devices at the time of the accident. The threat information was gathered from three sources: devices' manufacturer specifications, FCC limits, and ANSI C63.18-1997 for typical transmitters. The goal was to establish a reasonable bound of the RF emissions from typical PEDs devices. A summary of the data is shown in Fig. 2.

A. Manufacturer Specifications

Operating frequencies and the maximum radiated power were compiled for about 50 devices. They included portable radios, wireless phones, satellite phones, wireless local-area-network (LAN) devices, and two-way pagers [3].

B. Determination of FCC Limits

FCC limits were of interest since they provided an upper bound for commercially available devices. However, an extensive search through the FCC regulations proved tedious. As a result, the data shown in Fig. 2 were far from complete, and were limited to wireless phones and handheld transceivers.

C. ANSI C63.18-1997

This standard [4] recommended a practice for testing medical devices to specific RF transmitters. It also provided a good summary of typical transmitting PEDs. A partial list of PEDs is shown in Table 1 and the data plotted in Fig. 2.

D. Transmitting PEDs Threat Summary

Fig. 2 shows most devices radiate six watts or less, except at 27 MHz and at 900 MHz. The FCC limit at 27 MHz is 25 W for remote radio control, and the ANSI C63.18 standard shows 10 W maximum for radio modem at 900 MHz.

Fig. 2 also shows that PEDs frequencies were mostly between 25 MHz and 2.6 GHz (1996-1998 time frame). The FCC also allocates spectrum up to about 6 GHz for a few applications. Based on these data, the subsequent aircraft coupling measurements were chosen to range between 25 MHz and 6 GHz. Details about the coupling measurements are described in the next section.

TABLE I. PEDs and Maximum Output Power from ANSI C63.18-1997

Products	Frequency (MHz)	Power (W)
Hand-held transceivers	27, 49, 138-470	5
Wireless LANs	912, 2400	0.1
Personal digital assistants	896-940	4
Radio modems	896-901	10
Cellular Telephones	800-900	0.6
Personal satellite telephones	1610-1626.5	1
Licensed PCS equipment	1850-1910	1

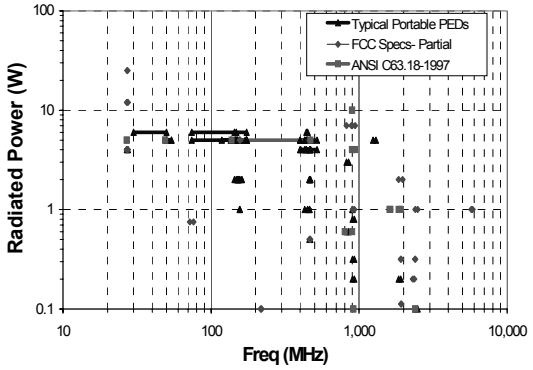

Figure 2. PED emission levels.

IV. RF Coupling to Fuel Tank and Wiring

There were three assumed paths for coupling RF energy to a fault location in the fuel tank:

- *Conducted Coupling:* Once coupled onto the FQIS wiring, RF power stayed attached to wiring all the way to the fault location to create a spark/arc.
- *Radiated Coupling:*
  - *Through FQIS Wiring*: RF power coupled into the CWT through the wiring then re-radiated. The energy then coupled onto the wiring near the fault location.
  - *Not through FQIS Wiring*: RF fields coupled into the CWT through other means such as pipes and unshielded apertures. The energy then radiated and coupled onto the wiring near a fault location to create a spark/arc.

It was desirable to measure and bound the power coupled into the CWT and its wiring of the aircraft. This was performed by measuring the induced power on the FQIS wiring at the CWT connector and the radiated power density in the CWT. A log-periodic antenna and a dual-ridge-horn antenna were used from 25 MHz to 6 GHz to simulate radiating PED sources in the passenger cabin.

A. Conducted Coupling to CWT on FQIS wiring

The FQIS wiring provided a conducted coupling path into the CWT. The coupling measurement was performed at the FQIS CWT connector, with an antenna in the passenger cabin simulating the internal PED sources.

This work was supported by the National Transportation Safety Board and the Aviation Safety Program Office at NASA Langley Research Center, Hampton, VA.

1) Test Method

Power coupled onto the FQIS was measured at the fuel tank connector, shown in Fig. 3. Due to the limited time available, the measurements were performed for only three pin combinations that represent both differential and common mode couplings: 1) HI Z to LO Z pins, 2) HI Z to LO Z COMP, and 3) all pins (HI Z, LO Z and LO Z COMP) tied together relative to airframe chassis.

The set up is shown in Fig. 4. A spectrum analyzer was used to measure the peak coupled power onto the FQIS wiring. A tracking sources delivered a fixed RF power level to the transmit antenna while performing synchronized frequency sweeps with the spectrum analyzer.

Fig. 5 illustrates the measurement being performed. The transmit antenna was scanning the length of the FQIS wiring directly under the floor. 5-10 centimeters spacing was maintained. Measurements were performed for both transmit antenna polarizations, parallel and perpendicular to the wiring.

The transmit antenna was also pointed in several random directions for identifying possible other coupling paths than through the FQIS wiring. However, random direction data show much lower coupling value in comparison.

2) Test Results

Fig. 6 shows the results from the aircraft measurement. Data are presented in two plots due to two separate hardware set-ups necessary to cover the frequency range of interest.

Of the three measurements, the All-Pins-to-Chassis measurement shows the highest coupling up to about 2 GHz. This configuration represents the common mode coupling, as oppose to differential mode coupling for the remaining measurements. Above 2 GHz, all three measurements show similar coupling envelope.

It is noted that the transmit antenna was used out-of-band below 100 MHz, resulting in high reflected power due to antenna mismatch. To simulate full radiated power, the measurement data were numerically scaled using a scale factor computed from the antenna's reflection coefficients. This approach was used in the past with good results [3][5].

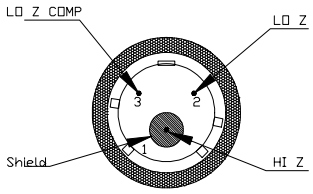

Figure 3. FQIS CWT Amphenol D3 connector schematic.

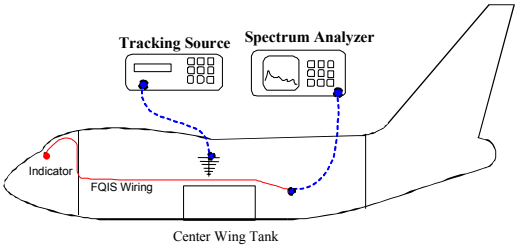

Figure 4. RF Coupling to FQIS wiring measurement.

Figure 5. A log-periodic antenna simulating a portable transmitter

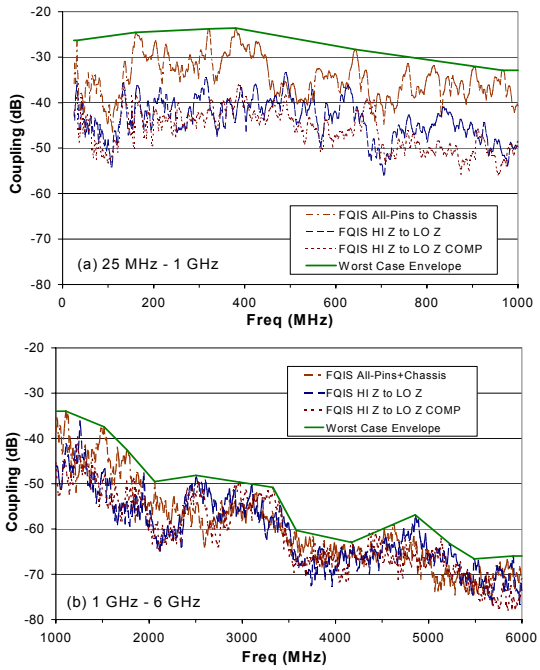

Figure 6. Coupling from passenger cabin to FQIS wiring.

A variation of this technique was also used to account for the impedance mismatch caused by the custom adapter. This custom adapter allowed measurement of power on the FQIS wiring using a 50-ohm N connector. The reflection coefficient from the interface was first measured and time-gated using a network analyzer. A simple mathematic manipulation allowed the correction factor to be derived. Without this correction, the mismatch errors can be as much as 4 dB at 25 MHz. Details on this correction factor derivation can also be found in [3].

B. Radiated Coupling to Antenna inside CWT

If the wiring is long relative to a wavelength, much of the coupled RF power on the FQIS wiring may be radiated. There is a possibility that some of the radiated energy may be coupled back onto the FQIS near a fault location. An arc/spark may result if there is sufficient energy. This section describes the measurement of *radiated power* in the CWT due to PED sources in the passenger cabin.

1) Test Method:

The measurement approach was similar to that used in measuring the coupling onto the FQIS wiring, but with antennas to measure the power density in the CWT. A mechanical stirrer was set up in the CWT bays to allow

measurements of field statistics, such as the peak power density. The set up is illustrated in Fig. 7.

Due to time restrictions, radiated field measurements were performed in only three of the six bays, labeled as Bays 1, 3 and 6 in Fig. 8. The same measurements were also repeated with the FQIS connector de-mated from the tank for comparison. A pre-amplifier was necessary above 1 GHz for the required instrument sensitivity, especially when the connector was de-mated.

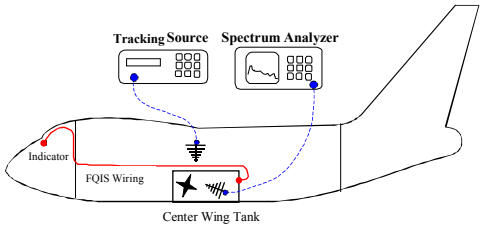

Figure 7. Radiated field coupling to CWT

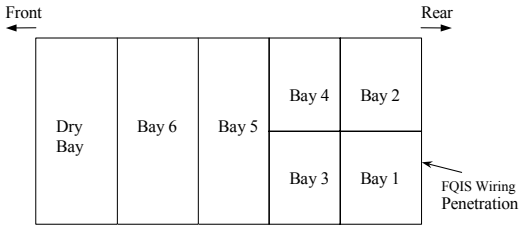

Figure 8. CWT top view representation. Data collected for Bays 1, 3 and 6.

The antennas used were expected to be more efficient in coupling RF energy than the FQIS wiring. As a result, the measurement provided an upper bound of the power that can be re-coupled onto the FQIS wiring or other structures.

The log-periodic antenna in the CWT was used out-of-band below 200 MHz. Unlike the transmit antenna in the passenger cabin, no corrections were applied in this case. The antennas were situated in tight spaces made of conducting surfaces. The cavity effects on antenna mismatch were difficult to quantify. It was decided best to present the data without the correction.

2) Test Results:

a) With FQIS Connector Mated to the Tank:

The results are shown in Fig. 9. The figure shows the coupling to Bay 1 (where the FQIS entered the CWT) dominates between 500 MHz to 2 GHz, while the coupling to Bays 3 and 6 dominated above 3 GHz. The worst-case coupling was at about 500 MHz, with approximately -43 dB coupling factor. This value was about 20 dB lower than the worst case coupling onto the FQIS wiring.

b) With FQIS Connector De-Mated:

For frequencies below 1.5 GHz, the peak coupling into the CWT was lowered by about 10 dB on the average when the FQIS connector was de-mated. This result shows that the FQIS wiring was the major contributor to the radiated field environment in this frequency range. Above 1.5 GHz, there were no significant differences in the envelopes, whether the connector was mated or de-mated. Further information on this result can be found in [3].

V. PEDs Coupled Power onto FQIS Wiring and Antenna in the CWT

Application of the PED threat levels in Fig. 2 to the peak coupling data envelopes in Fig. 6 and Fig. 9 resulted in Fig. 10 and Fig. 11, respectively. Fig. 10 shows the maximum PEDs power coupled onto the FQIS wiring, measured at the tank entry point. Fig. 11 shows the maximum power coupled into an antenna in the fuel tank, measured in Bays 1, 3 and 6.

Fig. 11 shows that the peak PEDs power coupled into an efficient antenna in the fuel tank (radiated field coupling) is approximately 0.2 milliwatt (mW) near 500 MHz. This result bounds the maximum radiated power in the fuel tank that could be coupled onto an internal structure or wiring through the radiated coupling path. Laboratory testing indicated that this level could not cause an arc/spark, even if there were faults in the wiring.

Fig. 10 shows at least 20 dB more power was measured at the FQIS wiring connector, however. The peak coupled power was about 60 mW near 27 MHz, and 20 mW between 100 to 500 MHz.

It was also evident from Fig. 10 and Fig. 11 that PEDs coupling at frequencies above 1 GHz declines significantly. This result was important for determining the upper frequency limit for subsequent laboratory testing.

The next section describes the laboratory testing to determine the minimum required power at the connector for an arc/spark condition. The safety margin was then determined from the data in Fig. 10 and the laboratory test results.

VI. Additional Fuel Tank Measurement

Fuel tank radiated field bay-to-bay coupling measurements were also made. The details are not reported here due to page length restrictions, but can be found in [3]. It can be summarized that there is strong field coupling between the fuel tank bays. At several frequencies, the coupling between two antennas in two adjacent bays was as strong as though the antennas were in the same bay. This result indicates that any RF leakage into one bay can result in similar field strength in adjacent bays. The leakage mechanisms were thought to be apertures (for fuel transfer), re-radiation via the FQIS wiring and conductive pipes. In these bay-to-bay coupling measurements, mechanical stirrers were used in each bays similar to the methods described in [6][7].

VII. RF Susceptibility Laboratory Testing

The FQIS wiring and the fuel level sensors were disassembled from the aircraft fuel tank for laboratory installation. The sensors were mounted on a large aluminum panel, with wiring-to-panel spacing similar to actual aircraft installation.

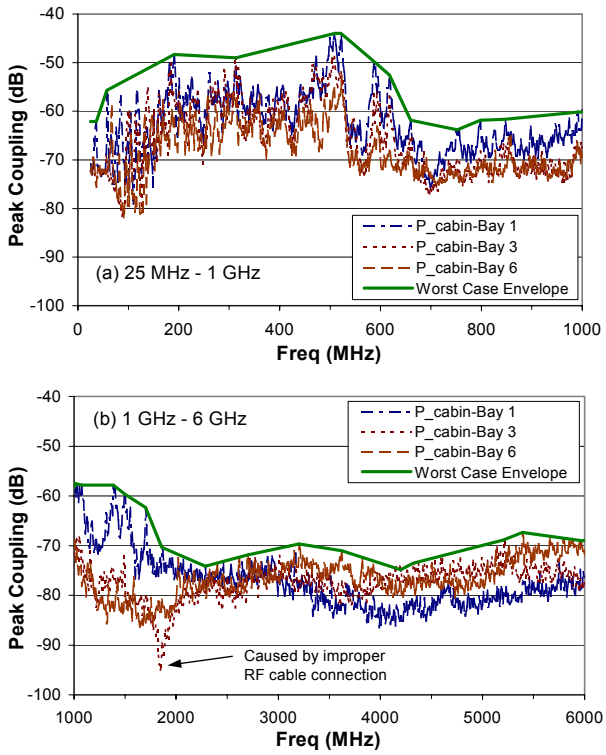

Figure 9. Peak coupling to antenna in different CWT bays.

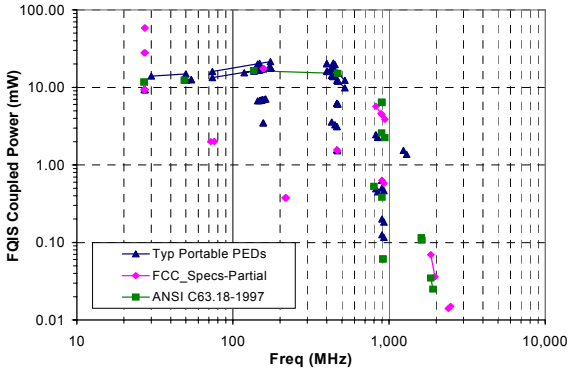

Figure 10. PEDs power coupled onto FQIS wiring.

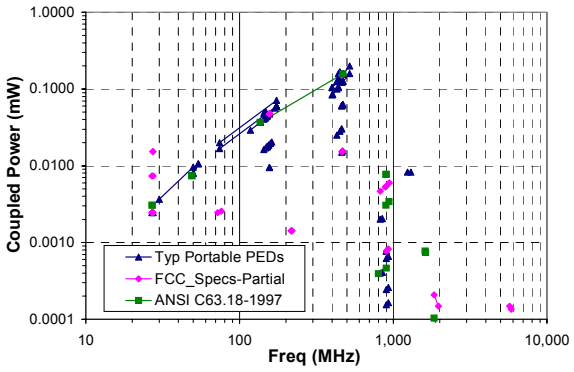

Figure 11. PEDs power coupled into an antenna in CWT.

Measurements were conducted to determine the location on the wiring that showed the largest voltage/current coupling gain relative to the connector location. At this location, a wiring fault was simulated by intermittently shorting the terminal to the chassis (accomplished by with a piece of bronze wool blown by modulated air jet). The fault was to simulate conducting debris floating in the fuel tank that could intermittently short the terminals. Without this fault simulation, it was not possible to create an arc/spark event with the available 40 W RF amplifier. Fig. 12 shows the simulated fault location and the setup. Fig. 13 illustrates the simulation of intermittent fault at the wiring.

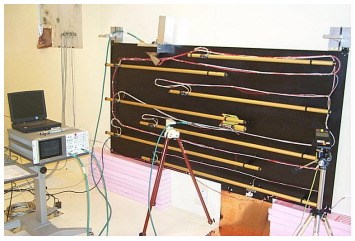

Figure 12. Laboratory set-up for arc/spark tests.

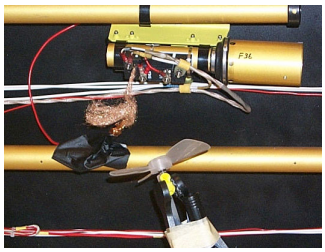

Figure 13. Air jet, modulated with a fan, causing intermittent short circuit between a wire terminal and the chassis.

A. Arc/Spark Detection

A critical element in the laboratory simulation is the ability to detect an arc/spark. Several methods were explored, including a night-vision scope attached to a consumer-grade camcorder, as shown in Fig. 14. Also considered were a nitrogen-cooled thermal imaging system for heat detection, a ultraviolet radiation detector with latched-alarm, and an AM radio to amplify static noise generated by an arc/spark. It was determined that the night-vision setup provided the best detection reliability (high detection rate with low false alarm), and was used for subsequent testing. A thermal imaging system was also setup for observation. However, no excessive heating was observed.

The arc/spark detection system must be capable of detecting an arc/spark having the energy content of about ¼ millijoule (mJ) or lower. Generally, ¼ mJ per spark is an industry accepted level below which the energy level is insufficient to ignite the fuel vapor [8].

The detection system must be calibrated to ensure the required sensitivity for avoiding missed detection. An electrostatic-discharge (ESD) gun was used to provide the arc/spark energy level for the calibration. A conservative calculation provided the voltage setting on the ESD gun for a ¼ mJ maximum discharge.

The night vision detection system reliably detected the arc/spark. An example image of the arc/spark event at the

simulated fault location, and the detected image through a night vision system are shown in Fig. 16. This image was taken during an actual test in which RF was injected into the connector causing the arc/spark at the simulated fault location.

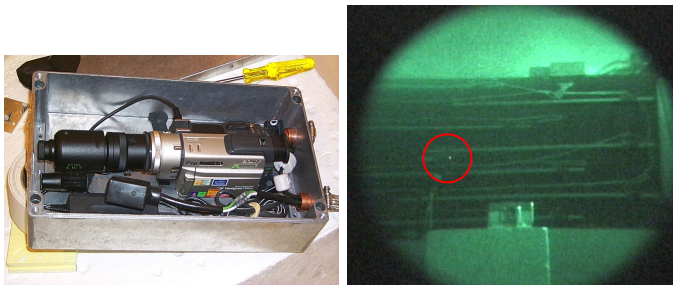

Figure 14. Night vision spark detection system and a detected spark (image reversed as seen through a mirror)

B. *Radiated Field Susceptibility*

As a result of the low coupled power to the receive antenna in fuel tank shown in Fig. 11, laboratory testing for radiated field susceptibility was very simple. Using a reverberation chamber and performing chamber calibration, the input power to the transmit antenna can be easily determined to achieve the same peak receive power shown in Fig. 11. Exposing the rest of the FQIS wiring to the same field did not result in arcing/sparking. The system was over-tested slightly up to the maximum level provided by a laboratory RF source, and no arc/spark was observed. The system was not tested to failure, however.

C. *Conducted Power Susceptibility*

The power determined to exist on the wires from PED sources, as shown in Fig. 10, was injected directly on the wires at the FQIS connector. No arcing/sparking events were observed during the test. However, under simulated fault conditions and with increased injected power, arcing/ sparking events at the fault location were observed.

In this test, up to 40 watts of RF power were injected onto the FQIS wires at the connector, while the simulated fault locations were monitored for arcing/sparking events. The required powers for an arc/spark event are shown in Fig. 15. Also shown in Fig. 15 are the previously determined maximum PEDs power levels at the connector. Additional details on the testing are presented in [3].

D. *Safety Margin Analysis*

Fig. 15 shows that the power required to create an arc/spark far exceeded the worst case PEDs power coupling onto the FQIS wiring by a large margin. Even with a 25 W PED transmitter at 27 MHz, the safety margin was about 10 dB. This result translates into approximately 250 W of PED power to cause an arc/spark, even with faulty wiring. Between 200 MHz to 300 MHz, the safety margin was about 18 dB. Above 300 MHz, a 40 W amplifier was not able to create an arc/spark.

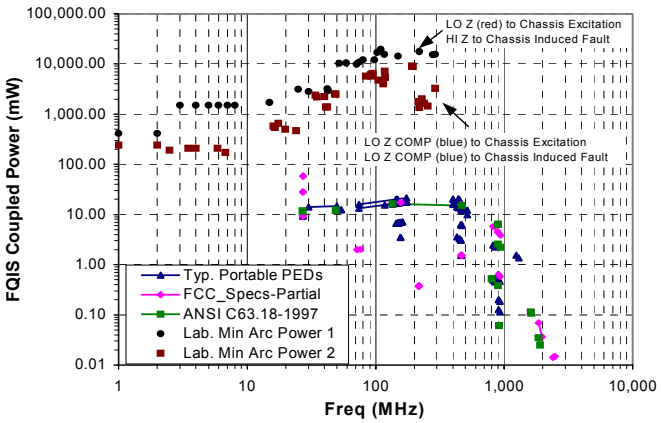

Figure 15. Adjusted PED threats on FQIS wiring. Also shown are FQIS minimum observed arc/spark levels with different excitation and induced faults.

VIII. Summary and Conclusion

This paper described the RF coupling measurements from PEDs in the passenger cabin of a large transport aircraft to its fuel tank and wiring. Laboratory simulations were also conducted to determine the power requirement for creating arcing/sparking events on the fuel tank wiring. Comparison of the two data sets resulted in the safety margin.

The FQIS wiring was determined to be the dominant coupling path for RF power into the fuel tank. There was a minimum of 10 dB safety margin between the power level required for a spark/arc and the power available from transmitting PEDs, even with a 25 W PED source at 27 MHz. A spark/arc within the fuel tank would require in excess of 250 watts from a single PED, or from multiple PEDs with frequencies and positions such that the effects are additive. This was assuming certain fault conditions existed on the wiring inside the fuel tank.

References

[1] Scarry, Elaine, 4/9/1998, "The Fall of TWA-800: The Possibility of Electromagnetic Inter-ference", The NY Review of Books, pp. 59-76.

[2] Macrae, M., D. Hughes, 1/1999, "TWA Flight 800 Electromagnetic Environment", United States DoD JSC Report JSC-CR-99-006.

[3] Ely, J. J., T. X. Nguyen, K. L. Dudley, S. A. Scearce, F. B. Beck, M. D. Desphande, and C. R. Cockrell, Mar. 2000, "Investigation of Electromagnetic Field Threat to Fuel Tank Wiring of a Transport Aircraft," NASA/TP-2000-209867.

[4] ANSI C63.18-1997 "Recommended Practice for an On-Site, Ad Hoc Test Method for Estimating Radiated Electromagnetic Immunity of Medical Devices to Specific Radio-Frequency Transmitters."

[5] Ladbury, J., G. Koepke, D. Camell, Jan. 1998, "Evaluation of the NASA Langley Research Center Mode-Stirred Chamber Facility," NIST Technical Note 1508.

[6] Crawford, M. L. and G.H. Koepke, Apr. 1986, "Design, Evaluation, and use of a Reverberation Chamber for Performing Electromagnetic Susceptibility/ Vulnerability Measurements," NBS Tech. Note 1092.

[7] Hatfield, M. O., Aug. 1988, "Shielding Effectiveness Measurements using Mode-Stirred Chambers: A Comparison of Two Approaches," IEEE Trans. on Electromagnetic Compatibility, Vol. 30, No. 3.

[8] Fisher, F. A., J. A. Plumer and R. A. Perala, *Lightning Protection of Aircraft*, Lightning Technologies Inc., 1990, p. 174.